NASA Technical Memorandum 101076

An Airfoil Pitch Apparatus – Modeling and Control Design

Daniel R. Andrews

March 1989

National Aeronautics and Space Administration

NASA Technical Memorandum 101076

An Airfoil Pitch Apparatus – Modeling and Control Design

Daniel R. Andrews, Ames Research Center, Moffett Field, California

March 1989

National Aeronautics and
Space Administration

Ames Research Center
Moffett Field, California 94035

AN AIRFOIL PITCH APPARATUS
Modeling and Control Design

Daniel R. Andrews
NASA Ames Research Center
Moffett Field, CA 94035

ABSTRACT

The study of dynamic stall of rapidly pitching airfoils is being conducted at NASA Ames Research Center. Understanding this physical phenomenon will aid in improving the maneuverability of fighter aircraft as well as civilian aircraft. A wind tunnel device which can linearly pitch and control an airfoil with rapid dynamic response is needed for such tests.

To develop a mechanism capable of high accelerations, an accurate model and control system is created. The model contains mathematical representations of the mechanical system, including mass, spring, and damping characteristics for each structural element, as well as coulomb friction and servovalve saturation. Electrical components, both digital and analog, linear and nonlinear, are simulated. The implementation of such a high-performance system requires detailed control design as well as state-of-the-art components.

This paper describes the system model, states the system requirements, and presents results of its theoretical performance which maximizes the structural and hydraulic aspects of this system.

INTRODUCTION

Assorted studies have investigated dynamic stall and its relation to rapidly pitching airfoils. Results indicate that pitch angles significantly beyond the static stall angle can be reached with large excursions in lift and pitching moment. The large excursions in lift and pitching moment are, in fact, the primary limiting factors in the performance of many aircraft (1).

Previous airfoil pitching mechanisms have achieved pitch rates of 800 deg/sec at an average power of 0.6 hp. The required dynamics of the present experiment are 3600 deg/sec at an average power of 10 hp with peak power exceeding 40 hp. To perform the required tests with an airfoil, the pitching mechanism must meet the following maximum dynamic parameters:

pitch angle, 0-60°
velocity, 3600°/sec
acceleration, 600,000°/sec^2
acceleration time, 0.006 sec
acceleration angle, 10°

The large acceleration required at Mach 0.5 airflow necessitates a powerful prime mover, or energy source. Detailed discussion of the prime mover selection will be omitted in this paper; however, an agile, high-performance hydraulic system provided the best power and response for its physical size. The emphasis of this discussion will be on control-system modeling and design. This discussion will include control theory and mathematical device modeling, followed by appropriate Bode and root locus plots to demonstrate system performance. The design was accomplished using the control system analysis program MATRIXx/System Build (Integrated Systems Incorporated). Each of the system components will be represented by a mathematical model, or transfer function, expressed in the complex frequency domain. Time-dependent solutions will be presented in the form of response plots.

CONSTANT PITCH RATE ACTUATOR

The actuator is shown in Figure 1 installed on the wind tunnel test section. The airfoil is mounted between two glass disks which rotate about the quarter cord of the airfoil. Glass disks provide optical access for measuring the vortices developing across the airfoil's surface.

The actuator is composed of a hydraulic servovalve, cylinder, and truss structure. A hydraulic servovalve operates a cylinder which pulls on a truss structure. The truss reacts on a bellcrank which pulls connecting links vertically, thereby pitching the glass disks and the airfoil. The torsion tube in the bellcrank is needed to minimize the torsional moment across the small airfoil. The NACA 0012 profile airfoil to be used is small (9.8 × 3.0 in.); therefore, the slightest twisting moment across the airfoil will disrupt the developing vortices.

SYSTEM MODELING

To study the feasibility and eventually maximize the pitching mechanism, a model representing the physical components is created. This model includes electrical components such as the transducers, motion controllers (digital and analog), and the software routines contained within the digital controller. The mechanical structure is modeled to include mass, spring, damping characteristics, and coulomb friction. Finally, the hydraulic properties of the cylinder and servovalve are represented. Many system components are represented by nonlinear models; examples include the signal quantization of digital to analog converters (DACs), pressure versus flow characteristics of valves, and potential saturation of the controller command signals. The entire system model is shown in Figure 2, and will be referred to in the discussion of the modeling and control system design.

STRUCTURE

Figure 3 shows the structural model of the pitching mechanism. The model was simplified by assuming the cross-member

spring constants were large enough to be rigid and, therefore, neglected. The structural model can then be simplified to a single energy transmission path. Reflecting the parameters to the prime mover (cylinder), to eliminate coupling of the individual structures, will allow us to solve for the key transfer functions defining the equations of motion:

$$\frac{\text{Cylinder Velocity}}{\text{Force Input}} = \frac{\dot{X}_1}{F}$$

$$= \frac{42.8}{S} \frac{\left(\begin{array}{r} [S^2 + 2(0.05)(15.5*10^3)S + (15.5*10^3)^2] \\ \times [S^2 + 2(0.05)(4140)S + (4140)^2] \end{array} \right)}{\left(\begin{array}{r} [S^2 + 2(0.03)(15.7*10^3)S + (15.7*10^3)^2] \\ \times [S^2 + 2(0.03)(5680)S + (5680)^2] \end{array} \right)}$$

$$\frac{\text{Window Position}}{\text{Cylinder Position}} = \frac{O_L}{X_1}$$

$$= \frac{1.45*10^{15}}{S} \frac{1}{\left(\begin{array}{r} [S^2 + 2(0.05)(15.5*10^3)S + (15.5*10^3)^2] \\ \times [S^2 + 2(0.05)(4140)S + (4140)^2] \end{array} \right)}$$

$$\frac{\text{Window Position}}{\text{Force Input}} = \frac{O_L}{F}$$

$$= \frac{61.9*10^{15}}{S^2} \frac{1}{\left(\begin{array}{r} [S^2 + 2(0.03)(15.7*10^3)S + (15.7*10^3)^2] \\ \times [S^2 + 2(0.03)(5680)S + (5680)^2] \end{array} \right)}$$

Notice the poles in O_L/X_1 cancel with the zeros in $\dot{X}_1/F$. This property is important in the design of the control system, since it enables closing an inner loop (velocity) with zeros in the structure thereby aiding in stability. The total combined structure transfer function is defined as O_L/F.

HYDRAULIC SYSTEM

The cylinder model and fluid compressibility can now be incorporated into the system model. In the hydraulic system, all fluid lines must be rigid and line lengths must be minimized to reduce compressibility and system compliance, as well as to account for entrained air in the hydraulic fluid.

$$\frac{P \text{ (lb/in.}^2\text{)}}{Q \text{ (in.}^3\text{/sec)}} = \frac{4(B)}{V_T} \frac{1}{S}$$

where B = Bulk Fluid Modulus (250,000 psi)
V_T = Total fluid compressed (27.8 in.^{3})
S = LaPlace operator

The cylinder converts hydraulic fluid flow into pounds of force:

$$\frac{F \text{ (lb)}}{P \text{ (lb/in.}^2\text{)}} = A$$

where A = Area of cylinder (in.^{2})

There is leakage in any hydraulic system and in this model it was estimated at 3% of the fluid flow. The leakage will alter the damping characteristics for the system.

$$\text{leakage} = \frac{(3\%)(Q \text{ in.}^3\text{/sec})}{\text{Available pressure}}$$

where Q = Average fluid rate = X_1*A
X_1 = Cylinder Velocity (188 in./sec)
A = Piston Area (2.36 in.^{2})

Additionally, there is back-velocity fluid flow which is the fluid expended in cylinder movement. The back-velocity loop subtracts from the available fluid flow, much like the back-EMF loop in a motor limits the current flowing through it. The back-velocity fluid flow is proportional to the speed of the cylinder. To drive the cylinder with suitable dynamic response, a high-performance servovalve must control the flow of fluid through the cylinder. The servovalve controller, internal servovalve feedback loops, and mechanical constraints of the servovalve must be modeled. The servovalve is modeled with a small-signal, second-order transfer function:

$$G_1(s) = \frac{K_s(W_n)^2}{S^2 + 2(z)(W_n)S + (W_n)^2}$$

where K_s = Power Spool Flow Gain ((in.^{3}/sec)/in.)
W_n = Frequency of servovalve (534 rad/sec)
z = Servovalve damping coefficient (0.70)

$$G_1(s) = \frac{4.28*10^9}{[S^2 + 2(0.7)(534)S + (534)^2]}$$

Servovalve damping (z) was estimated. To assure 0.70 damping is achievable, a bypass valve has been put in parallel with the cylinder to add leakage, as necessary, to increase servovalve damping. The servovalve has an internal position feedback loop closed with a linear velocity differential transformer (LVDT) on the first-stage valve spool. This is modeled as an equivalent gain, K_{LVDT}, while the servovalve amplifier is modeled as a gain, K_A (3).

$$K_{LVDT} = \frac{1}{K_D*K_X}$$

where K_D = LVDT Demodulator gain (V_{dc}/V_{rms})
K_X = LVDT Spool gain (V_{rms}/in.)

Finally, the first-stage valve spool has limited throw which will result in system saturation if stroke limits are reached. An important nonlinear effect of the servovalve/cylinder system, regeneration, must be modeled in a high-response system. The cylinder is an energy storage device, much like an electrical inductor is a current storage device. The energy of the cylinder is stored as momentum in both the piston and the hydraulic fluid. The flow through the cylinder cannot be changed instantaneously, and if an attempt is made, a pressure surge will ensue much like the voltage surge generated when open-circuiting an active inductor. A plot of the flow characteristics of a servovalve/cylinder system is shown in Figure 4, where

P_L = load (cylinder) pressure, P_s = supply pressure (3000 psi), Q_v = servovalve output flow, and x = first-stage valve spool position (3).

Four quadrants represent both positive and negative pressure, P_L, and positive and negative flow, Q_v. Quadrants 1 and 3 represent the "normal operation" regions where positive pressure creates positive flow, and negative pressure creates negative flow. Quadrants 2 and 4 represent the regeneration areas. In these quadrants the pressure may have reversed polarity, but the flow has not yet reversed. This situation occurs when the servovalve receives a command to rapidly change the flow direction through the cylinder. As the spool moves and rapidly halts flow in one direction, the pressure potential builds up until the cylinder fluid flow changes directions and enters back into quadrants 1 and 3.

At any flow rate there can be two different pressure values. The two equations shown below are used to approximate the previously discussed pressure/flow characteristics

$$Q > 0; \quad Q_v = K\sqrt{\frac{(P_s - P_L)}{P_s}}$$

$$Q \leq 0; \quad Q_v = K\sqrt{\frac{-(P_s + P_L)}{P_s}}$$

We, therefore, must have a switch in the model governed by the direction of fluid flow through the cylinder. This switch will choose between the two equations defining the regeneration characteristic. Note that the value received from the equations is normalized about full flow. For example, if the P_L versus Q_v calculated flow is 75%, the command flow in the model will be multiplied (attenuated) by 0.75 to reflect the pressure drop across the servovalve.

CONTROLLERS

A digital controller is used to control the pitch mechanism position loop, while an analog servovalve controller is used for the velocity loop. Because the desired motion of the airfoil is a ramp, the digital controller must have a ramp generator. The controller must also be able to calculate the difference between the commanded position and the actual position, which requires an equivalent summing junction in software. The controller has the capability of compensation in the form of a lead and lag filter. This capability enables placing a zero and/or pole into the position loop, as well as an integrator to help remove steady-state errors.

Because of the nature of digital control and the sampling of the analog system, there is an inherent time delay associated with the controller's operation. If the sampling rate is not suitably high, the time delay could be detrimental to the stability of the system and so it is modeled. The system is analog, so the digital controller must convert its output to the analog domain. A DAC performs the conversion which creates a quantized analog signal. The quantization could potentially excite a mode in the system and is important to model. The DAC also has a gain associated with it. The gain is a coupling ratio of counts in the digital domain to voltage in the analog world (6).

The output voltage from the DAC is fed to an analog voltage power amplifier which amplifies the signal sent to the servo controller. Because this system requires high dynamic response, it is possible that the power amplifier will saturate if the input signal exceeds ±10 V which must be included in the model. The analog command voltage is then fed into the velocity summing junction in the analog servovalve controller. A gain associated with the analog controller is shown after the power amplifier saturation block.

The final system models are the feedback elements consisting of a velocity transducer and a position transducer. The velocity transducer is a linear velocity transducer (LVT). The motion of a permanent magnet induces a voltage proportional to speed in the windings surrounding the magnet. The mathematical model is simply a gain. The LVT is mounted on the cylinder piston to take advantage of the structure zeros enclosed in the velocity feedback loop. The position transducer is an incremental encoder. The encoder converts angular position of the glass disks into digital pulses which are converted into counts in the digital position controller. Modeling of the encoder is similar to the DAC. A gain is associated with the encoder as angular position in radians is converted into counts in the digital domain. Because the analog position is being converted into the digital domain, a quantization block is also needed.

CONTROL ANALYSIS AND DESIGN

To begin the theoretical control system analysis and design, we must tune the innermost loop with all other loops opened. We can then close and tune each loop concentrically, until eventually all of the loops have been tuned. It is important to note that the tuning and analysis will be done with only the linear model blocks in place. By eliminating the nonlinear blocks, familiar, classical control techniques can be employed. After the optimal linear system has been achieved, the nonlinear blocks will be added in. These nonlinearities may cause problems with the "optimally tuned" linear system and further adjustments would then have to be performed.

Open-Loop Circuit ($\dot{X}_1/\tilde{Q}$):

This discussion begins with the cylinder, area, structure, and leakage feedback blocks of the system model. The theoretical poles and zeros of this system are shown below:

Zeros	Complex Roots	Frequency, rad/sec	Damping, z
Structure:	–777 ±j15,520	15,520	0.05
Structure:	–207 ±j4,140	4,140	0.05
Poles	**Complex Roots**	**Frequency, rad/sec**	**Damping, z**
Structure:	–472 ±j15,730	15,730	0.03
Structure:	–170 ±j5,670	5,670	0.03
Cylinder:	–425	425	1.0
Velocity integrator:	0	0	1.0

The structure poles are lightly damped, although at a high natural frequency, while the cylinder has a low natural frequency. To get the desired performance from the system, the cylinder frequency will have to be improved. The open-loop Bode plot of this system is shown in Figure 5.

Back-Velocity Loop ($\dot{X}_1/\tilde{Q}$):

The next loop to close is the back-velocity loop which feeds back the cylinder speed. The Bode plot is shown in Figure 6. The new system roots are shown below:

Zeros	Complex Roots	Frequency, rad/sec	Damping, z
Structure:	–777 ±j15,520	15,520	0.05
Structure:	–207 ±j4,140	4,140	0.05

Poles	Complex Roots	Frequency, rad/sec	Damping, z
Structure:	–460 ±j15,740	15,750	0.03
Structure:	–174 ±j6,050	6,050	0.03
Cylinder/ integrator:	–220 ±j1,960	1,970	0.11

The velocity integrator, which came from the $\dot{X}_1/F$ transfer function, combined with the cylinder pole and became a complex root pair at a higher natural frequency, which is achieved at the expense of cylinder damping. The lower frequency structure pole moved out to a slightly higher frequency, and the high-frequency pole did not move.

The next step is to add the servovalve with its associated LVDT loop and amplifier to the previous system. The open-loop Bode plot is shown in Figure 7. The resultant system frequencies are shown below:

Zeros	Complex Roots	Frequency, rad/sec	Damping, z
Structure:	–777 ±j15,520	15,520	0.05
Structure:	–207 ±j4,140	4,140	0.05

Poles	Complex Roots	Frequency, rad/sec	Damping, z
Structure:	–460 ±j15,740	15,750	0.03
Structure:	–174 ±j6,050	6,050	0.03
Cylinder/ integrator:	–220 ±j1,960	1,970	0.11
Servovalve:	–377 ±j378	534	0.70

Velocity-Feedback Loop ($\dot{X}_1/V$):

The velocity loop will force the cylinder to accurately track the velocity command. To appropriately choose the velocity loop gain, a root locus plot is created to track the poles' locations as a function of velocity loop gain. The loop gain must be increased in the velocity loop to increase the servovalve pole frequency and get the necessary performance from the servovalve. Notice, however, in the previous Bode plot, that the phase and gain margins are negative, indicating an unstable system with unity feedback in the velocity loop. The velocity-feedback transducer gain must, therefore, be less than unity. The root locus in Figure 8 confirms this assertion, showing the cylinder poles heading toward the right-hand plane as velocity-feedback gain approaches unity.

A feedback gain for the velocity transducer was chosen and the resultant roots are shown below:

Zeros	Complex Roots	Frequency, rad/sec	Damping, z
Structure:	–777 ±j15,520	15,520	0.05
Structure:	–207 ±j4,140	4,140	0.05

Poles	Complex Roots	Frequency, rad/sec	Damping, z
Structure:	–460 ±j15,740	15,750	0.03
Structure:	–174 ±j6,050	6,050	0.03
Cylinder/ integrator:	–212 ±j1,920	1,930	0.11
Servovalve:	–386 ±j587	703	0.55

Notice that the servovalve frequency was improved at the expense of damping. The Bode plot is shown in Figure 9. As stated previously, the velocity and position transducers are located in two different places. The difference in location of the transducers can be explained by looking at the transfer function, X_1/F. This transfer function has two zero pairs in the numerator of the transfer function. These zeros, enclosed in the velocity loop, tend to attract system poles, keeping the poles from entering the right-hand plane, and thereby becoming unstable. Because these poles are restrained, the velocity loop gain can be increased to get the velocity of the device to more accurately track the velocity command. If the velocity transducer had been put at the airfoil instead of the cylinder, the zeros would have been cancelled by the poles in the O_L/X_1 transfer function. The system poles would not then have been restrained to the left-hand plane. The velocity transducer is, therefore, located on the cylinder in the velocity-feedback loop, while the position loop transducer is located at the actual load, to assure that the airfoil arrives at its final position as desired.

Position Feedback Loop (O_L/C):

The lead and lag filters in the position loop of the digital controller are initially set to zero to best tune this system prior to compensation. The position loop gain was chosen to achieve the best dynamic response. In this case the servovalve poles are heading toward the right-hand plane, limiting the amount of position loop gain. Resultant roots are shown below:

Zeros	Complex Roots	Frequency, rad/sec	Damping, z
Structure:	–777 ±j15,520	15,520	0.05
Structure:	–207 ±j4,140	4,140	0.05

Poles	Complex Roots	Frequency, rad/sec	Damping, z
Structure:	–460 ±j15,740	15,750	0.03
Structure:	–174 ±j6,050	6,050	0.03
Cylinder/ integrator:	–247 ±j1,920	1,930	0.13
Servovalve:	–80.2 ±j608	613	0.13
Position integrator:	–544	544	1.0

It can be seen that the servovalve poles migrated toward the right-hand plane of the root locus, thereby decreasing the frequency and damping of that pole pair. The real pole is also at a low frequency, resulting in decreased system bandwidth. The Bode plot for the uncompensated position loop is shown in Figure 10.

Compensation (O_L/C):

The position controller software lead compensation can now be used to improve the damping of the servovalve. The zero is placed at 900 rad/sec, while the accompanying compensation pole is placed at 2000 rad/sec. The compensation integrator in the software will not be used. Although the integrator helps to

reduce steady-state error in the system, it also introduces a 90° phase lag which decreases phase margin and, therefore, system damping. The resultant root locus plot is shown in Figure 11. The system roots after compensation are shown below:

Zeros	Complex Roots	Frequency, rad/sec	Damping, z
Structure:	–776 ±j15,520	15,520	0.05
Structure:	–207 ±j4,140	4,140	0.05
Lead compensator:	–900	900	1.0

Poles	Complex Roots	Frequency, rad/sec	Damping, z
Structure:	–460 ±j15,740	15,750	0.03
Structure:	–173 ±j6,050	6,050	0.03
Cylinder/ integrator:	–248 ±j1,900	1,910	0.13
Servovalve:	–189 ±j639	666	0.28
Position integrator:	–297	297	1.0
Lag compensator:	–2.030	2,030	1.0

Improvement in the servovalve frequency and damping is noticeable. The servovalve natural frequency has been improved from 613 rad/sec to 666 rad/sec (10%), and the damping improved from 0.13 to 0.28 (115%). The Bode plot for the compensated position loop is shown in Figure 12.

Nonlinear Elements:

Now that the linear control system model has been tuned, the nonlinear model blocks can be inserted and the actual predicted results viewed. Various system responses are displayed in Figure 13. An important plot to note is the position controller amplifier where the output goes into saturation. When the position loop is saturated, the effect is to open the position loop feedback, giving the velocity-feedback loop control of the system. The response of the system is therefore determined by the poles in the velocity loop while the position loop is saturated.

The effect of this amplifier saturation can be seen in the plot of flow response. Upon close inspection, it can be seen that the frequency of the ringing at high-flow command is different from the ringing frequency at zero flow command. The frequency of oscillations during high flow, while the position controller is saturated, is 105 Hz;while at zero flow command the oscillation frequency is only 95 Hz. These ringing frequencies are determined by the natural frequency of the dominant pole(s) in the velocity and position loops, respectively. The servovalve is the dominant pole in both the velocity loop and the position loop. The output ringing frequency found during position controller saturation corresponds to the servovalve frequency in the velocity loop. The output ringing frequency found while the position controller was not saturated corresponds to the servovalve frequency in the position loop.

Note that in the pressure response plot, the pressure during acceleration reaches 900 psi, which is less than the deceleration pressure of 1300 psi. This difference demonstrates the back-velocity loop's ability to aid in stopping the cylinder motion. During the acceleration, the back-velocity loop is fighting the motion all the way, impeding the cylinder's ability to accelerate. During deceleration, the back-velocity loop is still trying to impede the motion of the cylinder, aiding in slowing the cylinder to a stop.

The high-frequency shaking occurring in the cylinder acceleration plot ($\ddot{X}$) appears to be one of the structure poles. The shaking frequency is approximately 1000 Hz which matches the lower frequency structural pole of 962 Hz. This plot indicates the potential for exciting some of the structure poles. However, in the position-response plot the shaking is integrated twice and dramatically reduced.

CONCLUSION

A system model encompassing a wide range of real-world effects showed the ultimate system design parameters of 60° pitch angle at 3600°/sec pitch rate can be theoretically achieved. The acceleration of the airfoil was within 0.006 sec and 10° of pitch angle. Although the required design performance was demonstrated, there is little room for improvement in the system response. All of the system variables were maximized for linearity of pitch rate, minimum overshoot, and appropriate acceleration rates.

ACKNOWLEDGEMENTS

The author would like to thank Reginald F. King, David A. Howe, Philip K. Snyder, and Roland Heikkinen of Ames Research Center for their comments and suggestions throughout the development of this project.

REFERENCES

(1) Carr, Lawrence W., "Dynamic Stall-Progress in Analysis and Prediction." U.S. Army Aeromechanics Laboratory, and NASA, Ames Research Center, 1988.

(2) Franklin, Gene, Powell, David and Abbas Emami-Naeini, Feedback Control of Dynamic Systems, Addison Wesley, Massachusetts, 1987.

(3) Thayer, W.J., Transfer Functions for Moog Servovalves, Technical Bulletin #103, Moog Inc., New York, 1965.

(4) DC Motors, Speed Controls, Servo Systems, Electro-Craft Corporation, 1980.

(5) D'Azzo, John J. and Houpis, Constantine, Control System Analysis and Synthesis, McGraw-Hill. New York and Toronto, 1960.

(6) Tal, Jacob, Motion Control by Microprocessors, Galil Motion Control Inc., 1984.

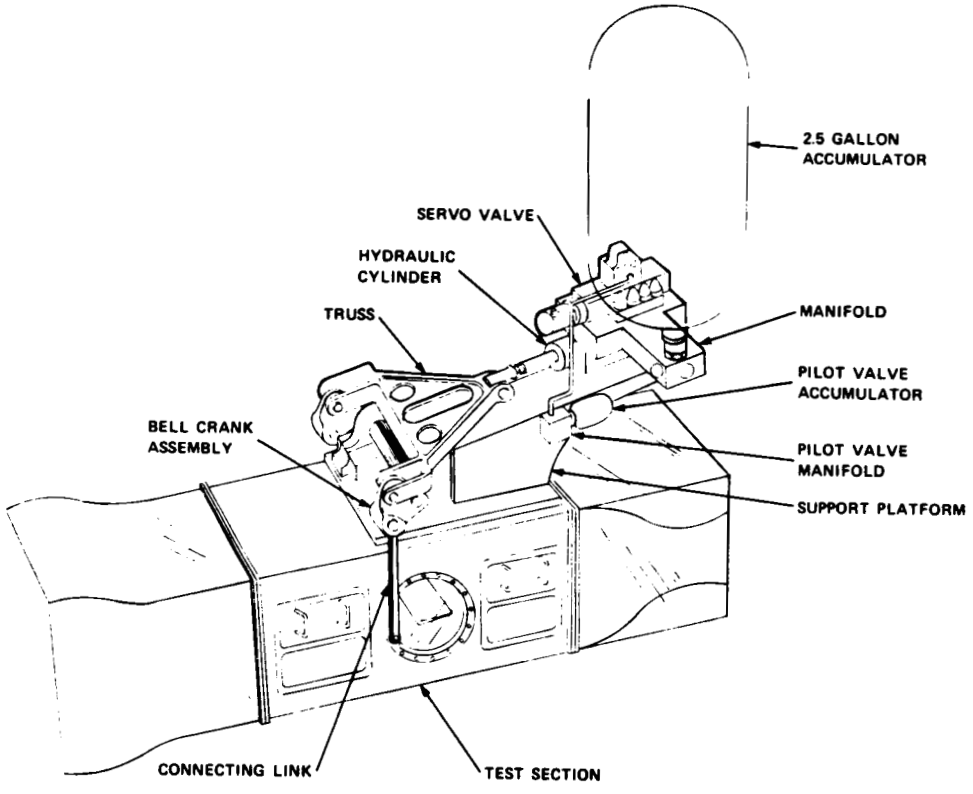

Figure 1 – Constant pitch rate apparatus.

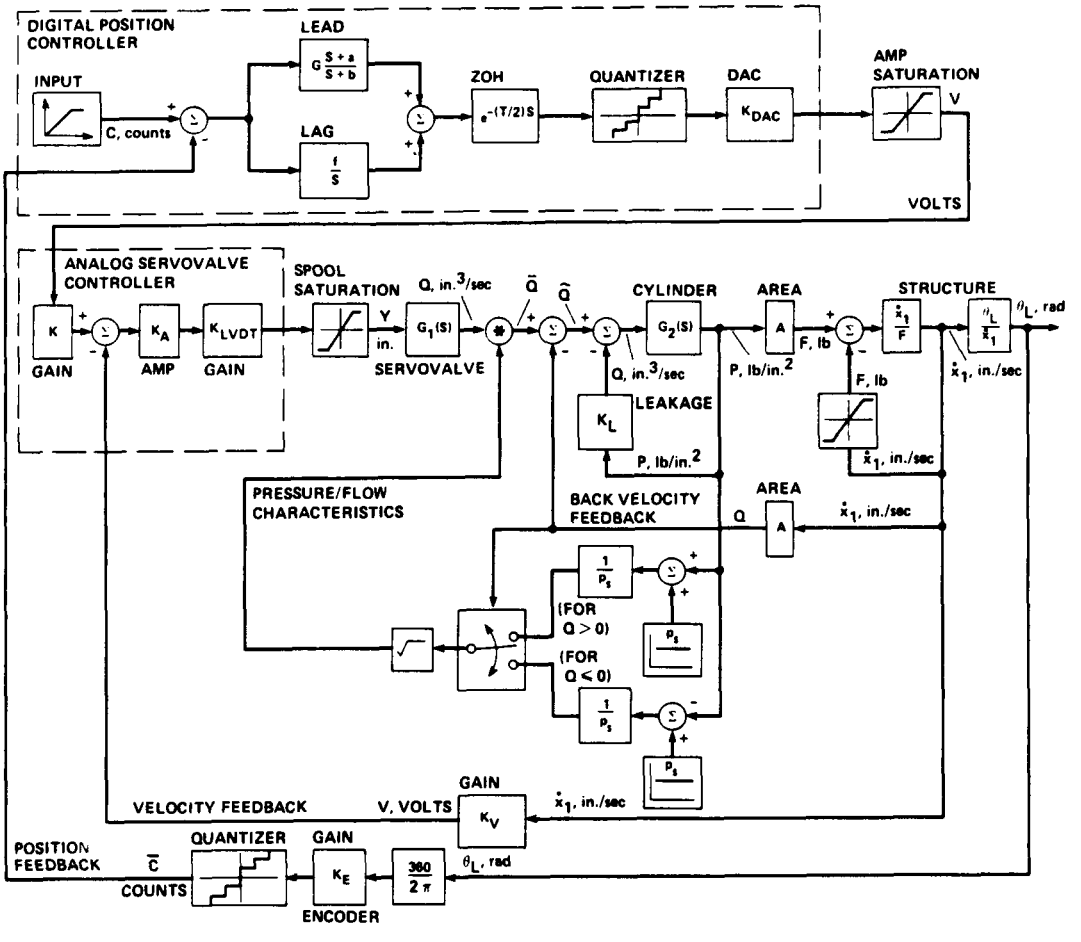

Figure 2 – Control system model.

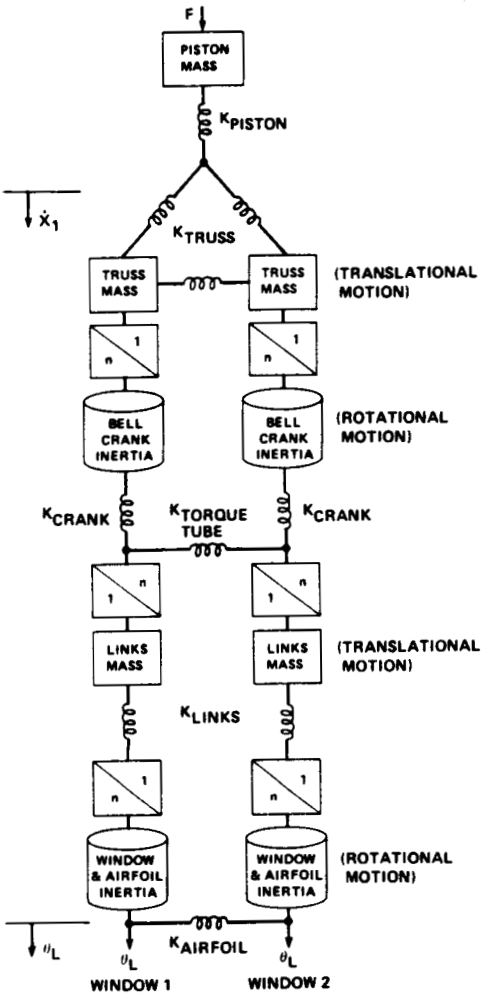

Figure 3 – Mechanical structure model.

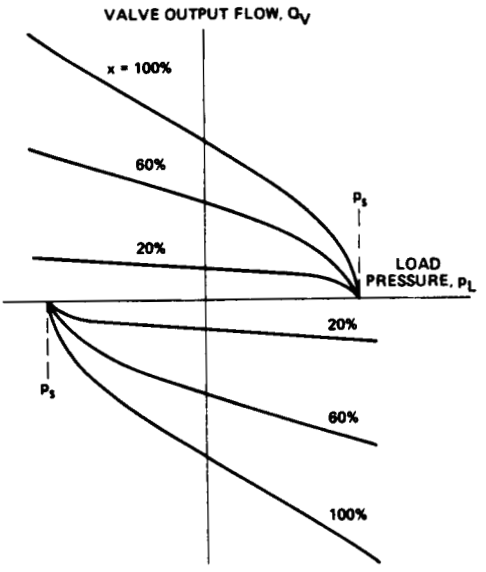

Figure 4 – Servovalve pressure-flow characteristics.

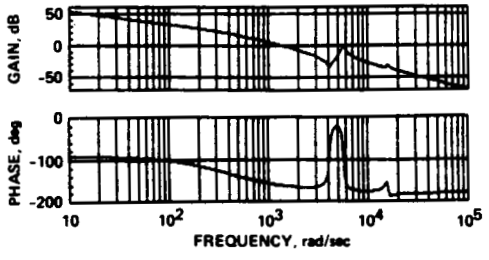

Figure 5 – Bode plot of open loop structure ($\dot{X}_1/\tilde{Q}$).

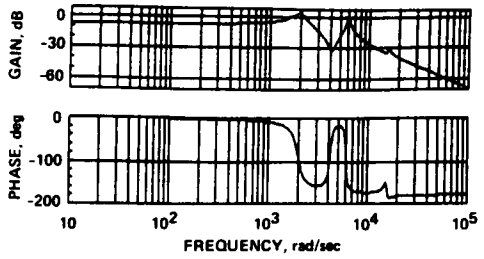

Figure 6 – Bode plot of back-velocity loop ($\dot{X}_1/\bar{Q}$).

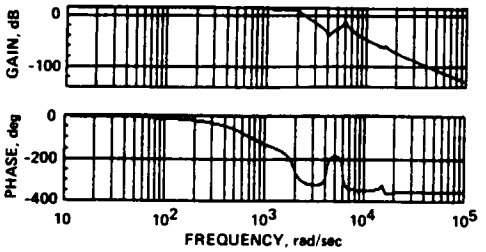

Figure 9 – Bode plot of velocity-feedback loop (X_1/V).

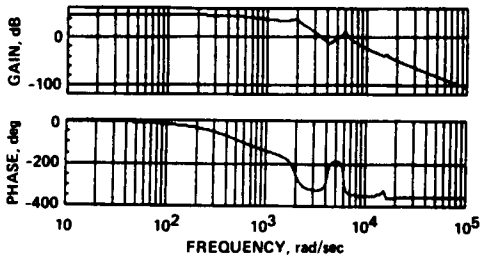

Figure 7 – Bode plot of structure and servovalve.

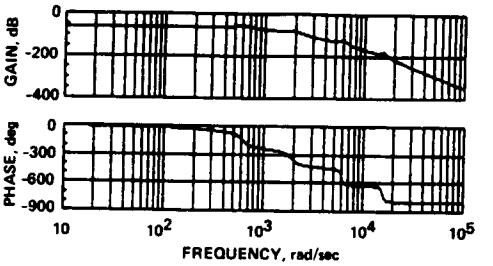

Figure 10 – Bode plot of uncompensated position loop.

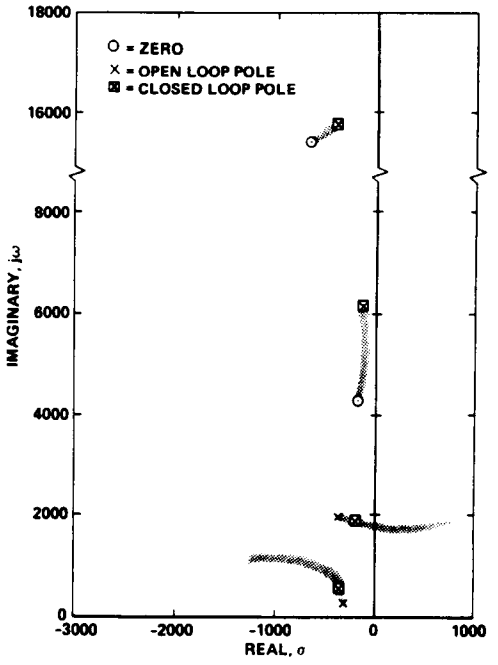

Figure 8 – Locus of roots for velocity feedback.

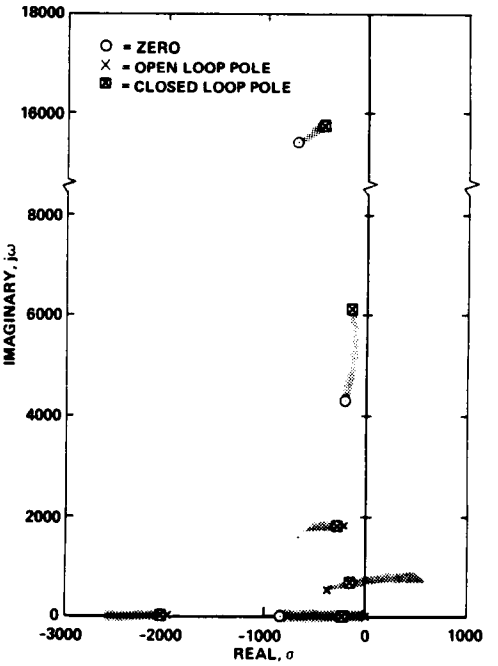

Figure 11 – Locus of roots for compensated position loop.

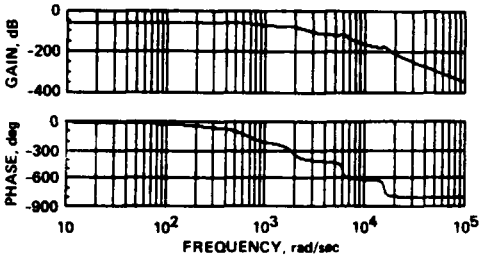

Figure 12 – Bode plot of compensated position loop.

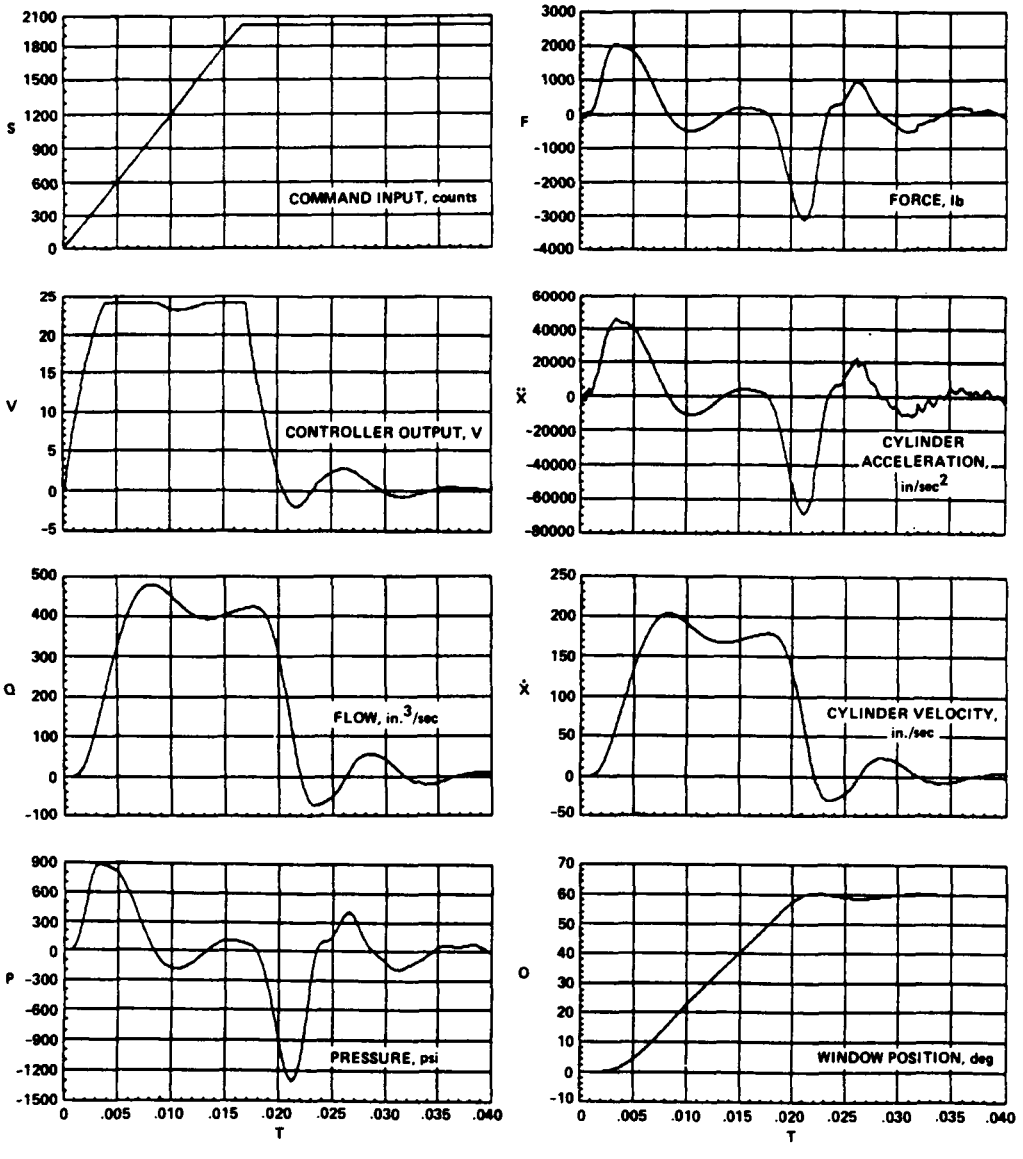

Figure 13 – System theoretical response plots.

NASA
National Aeronautics and Space Administration

Report Documentation Page

1. Report No.	2. Government Accession No.	3. Recipient's Catalog No.
NASA TM-101076		

4. Title and Subtitle

An Airfoil Pitch Apparatus–Modeling and Control Design

5. Report Date

March 1989

6. Performing Organization Code

7. Author(s)

Daniel R. Andrews

8. Performing Organization Report No.

A-89051

10. Work Unit No.

505-61-51

9. Performing Organization Name and Address

Ames Research Center
Moffett Field, CA 94035

11. Contract or Grant No.

13. Type of Report and Period Covered

Technical Memorandum

12. Sponsoring Agency Name and Address

National Aeronautics and Space Administration
Washington, DC 20546-0001

14. Sponsoring Agency Code

15. Supplementary Notes

Point of Contact: Daniel R. Andrews, Ames Research Center, MS 213-4, Moffett Field, CA 94035
(415) 694-4096 or FTS 464-4096

Submitted as a meeting paper for the Instrument Society of America 35th Instrumentation Symposium, Orlando, Florida, May 1-4, 1989.

16. Abstract

The study of dynamic stall of rapidly pitching airfoils is being conducted at NASA Ames Research Center. Understanding this physical phenomenon will aid in improving the maneuverability of fighter aircraft as well as civilian aircraft. A wind tunnel device which can linearly pitch and control an airfoil with rapid dynamic response is needed for such tests.

To develop a mechanism capable of high accelerations, an accurate model and control system is created. The model contains mathematical representations of the mechanical system, including mass, spring, and damping characteristics for each structural element, as well as coulomb friction and servovalve saturation. Electrical components, both digital and analog, linear and nonlinear, are simulated. The implementation of such a high-performance system requires detailed control design as well as state-of-the-art components.

This paper describes the system model, states the system requirements, and presents results of its theoretical performance which maximizes the structural and hydraulic aspects of this system.

17. Key Words (Suggested by Author(s))	18. Distribution Statement
Servo-hydraulic control system Airfoil pitch apparatus Control system modeling and design	Unlimited – Unclassified Subjct category: 33

19. Security Classif. (of this report)	20. Security Classif. (of this page)	21. No. of pages	22. Price
Unclassified	Unclassified	13	A02